Generation and characterization of millimeter-scale plasmas for the research of laser plasma interactions on Shenguang-III prototype*

Li Zhi-Chao(李志超)[a)b)], Zheng Jian(郑 坚)[a)†], Ding Yong-Kun(丁永坤)[b)], Yin Qiang(尹 强)[b)], Jiang Xiao-Hua(蒋小华)[b)], Li San-Wei(李三伟)[b)], Guo Liang(郭 亮)[a)b)], Yang Dong(杨 冬)[b)], Wang Zhe-Bin(王哲斌)[b)], Zhang Huan(章 欢)[b)], Liu Yong-Gang(刘永刚)[b)], Zhan Xia-Yu(詹夏宇)[b)], and Tang Qi(唐 琦)[b)]

[a)] *CAS Key Laboratory of Basic Plasma Physics, and Department of Modern Physics, University of Science and Technology of China, Hefei* 230026, *China*

[b)] *Research Center of Laser Fusion, China Academy of Engineering Physics, Mianyang* 621900, *China*

(Received 11 May 2010; revised manuscript received 14 June 2010)

In order to produce millimeter-scale plasmas for the research of laser-plasma interactions (LPIs), gasbag target is designed and tested on Shenguang-III prototype laser facility. The x-ray pinhole images show that millimeter-scale plasmas are produced with the gasbag. The electron temperature inferred from the stimulated Raman scattering (SRS) spectrum is about 1.6 keV. The SRS spectrum also indicates that the electron density has a flat region within the duration of 200 ps. The obvious differences between the results of the gasbag and that of the void half hohlraum show the feasibility of the gasbag target in creating millimeter-scale plasmas. The LPIs in these millimeter-scale plasmas may partially mimic those in the ignition condition because the duration of the existence of a flat plasma density is much larger than the growth time of the two main instabilities, i.e., SRS and stimulated Brillouin scattering (SBS). So we make the conclusion that the gasbag target can be used to research the large-scale LPIs.

Keywords: gasbag target, large scale, laser plasma interaction, stimulated Raman scattering

PACC: 5255M, 5250J, 5240D, 5235P

1. Introduction

Indirect-drive scheme of inertial confinement fusion (ICF) is one of the most promising ways to realize the goal of ignition.[1,2] In this scheme, laser energies have to be converted into thermal x-rays through a hohlraum and then to implode and ignite fuel capsules located at the centre of the hohlraum. In order to control the motion of the high-Z plasmas from the irradiated inner wall, the hohlraum has to be filled with low-Z gas.[1,2] Therefore, laser beams have to propagate a rather long distance (several millimeters) in uniform underdense plasmas before they reach the high-Z wall of the hohlraum and convert their energies into thermal x-rays. When the intense laser beams propagate in plasmas, complicated laser-plasma interactions (LPIs)[3] can occur. Various parametric instabilities[4−6] can be driven with the intense laser beams and profoundly affect the laser light propagations and the laser-hohlraum coupling efficiency. For example, stimulated Brillouin scattering (SBS)[7,8] and stimulated Raman scattering (SRS)[9,10] could scatter a large fraction of incident laser energy, significantly lower the conversion efficiency of laser energy into thermal x-rays, and then have harmful effect on the capsule implosion. It is now well recognized that LPIs in large scale plasmas must be carefully controlled in order to realize the ignition goal.[11]

The SRS and SBS instabilities have been investigated with the plasmas produced by laser beams irradiating high-Z planar targets[12] or cylindrical Au-wall hohlraums[13] in previous experiments. The plasmas generated with such targets are very different from the plasmas in the ignition condition. For example, the plasmas generated from a planar target freely expand into the vacuum and inherently have much smaller velocity and density scale lengths in comparison with those produced with a gas-filled hohraum target.[11]

*Project supported by the National Natural Science Foundation of China (Grant No. 10625523) and the Innovation Project of the Chinese Academy of Sciences (Grant No. KJCX2-YW-N36), and National High-Tech Program of China.

†Corresponding author. E-mail: jzheng@mail.ustc.edu.cn

© 2010 Chinese Physical Society and IOP Publishing Ltd

The laser-plasma instabilities in these experiments can also be quite different from those in the ignition condition due to the different plasma conditions.

In order to understand the physics of the parametric instabilities in the conditions relevant to ignition as close as possible with our present laser facility, a large uniform underdense plasma platform has to be built. Recently we have developed a method to create millimeter-scale uniform plasmas using a gasbag target which was first investigated by Denavit *et al.*[14] The gasbag contains a volume of gas with appropriate pressure so that the produced plasmas can have desired size and uniformity in the electron density and temperature. In this paper, we report the generation and characterization of the plasma produced by this gasbag target on Shenguang-III prototype laser facility.[15] For comparison, the experimental results from void half hohlraum[16] are also presented because such void half hohlraums are often used to study the hohlraum physics on Shenguang-III prototype. The analysis of the differences between the results of these two types of targets indicates the feasibility of the new gasbag target in creating millimeter-scale plasmas. In these millimeter-scale plasmas, the effect of the convection damping is mitigated and that of the daughter wave damping is dominant. The LPIs in these millimeter-scale plasmas can partially characterize the processes in the ignition condition, and the new gasbag target can be used to research the large-scale LPIs.

2. Target design and experiment arrangement

The gasbag target is made of two 0.4-μm-thick-polyimide films glued to a 400-μm-thick-steel washer whose inner diameter is 1600 μm. Gas is filled into the target through a thin tube mounted in the washer. With the pressure of the filling gas, the polyimide films are stretched and the overall diameter of the inflated gasbag is approximately 1 mm. The gasbag target is filled with 0.8 atm (1 atm=1.01325 $\times$ 10^5 Pa) of Xe gas, corresponding to an electron density of about 7.5×10^{20} cm^{-3} with the assumption that the average charge state of Xe is 40 when the gas is heated by the laser beams. Shown in Fig. 1 are the photographs of a typical gasbag target from side view (a) and top view (b).

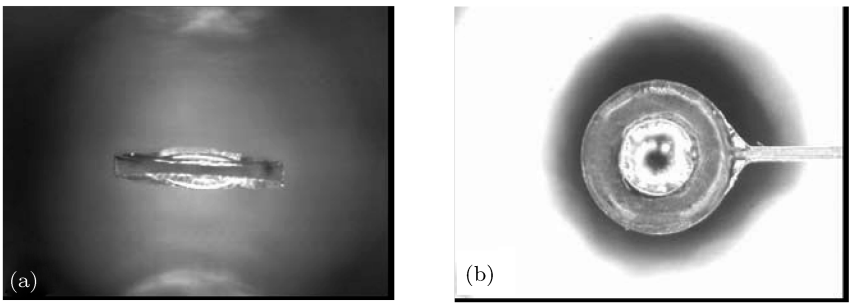


Fig. 1. Photographs of the gasbag target from (a) side view and (b) top view.

The experiments were performed on Shenguang-III prototype laser facility[15] at Research Centre of Laser Fusion. Eight frequency-tripled (351 nm) laser beams irradiated the target from upward in 45° cone with 1-ns pulse duration. Each beam delivered 600-J energy to the target. The interaction beam, the "S4" laser beam was delayed by 330 ps with respect to the other seven heater beams. Each incident laser beam is focused with an f/5.4 lens to the centre of the gasbag, which was placed horizontally in the chamber centre. The spot size on the surface of the target was about 400 μm$\times$400 μm and the nominal laser intensity was 4×10^{14} W/cm^2. Shown in Fig. 2 is the sketch map of the arrangement of the gasbag experiment. An x-ray pinhole camera (XPHC) is placed near the upper-pole axis and a full aperture backscatter system (FABS)[17] is installed at the interaction beam "S4". Via filtering through a 300-μm-thick Ti film and a 20-μm-thick Al film, the x-ray pinhole camera can take the images of x-rays with photon energy higher than 3 keV. Each pixel of the camera corresponds to about 4.3 μm of the spatial target size. The FABS contains the SRS

spectrum diagnosis with the temporal resolution of 100 ps.

The arrangement of the hohlraum experiment is almost the same as that of the gasbag experiment. The void half hohlraum[16] is a 1-mm diameter and 0.8-mm-long gold-wall cylinder with one 0.65-mm-diameter laser entrance hole (LEH). Eight laser beams irradiate the hohlraum wall from the LEH in 45° cone.

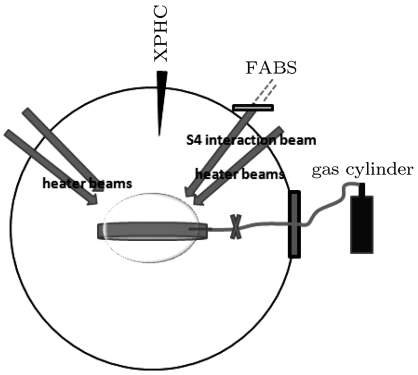


Fig. 2. Sketch map of the arrangement of the gasbag experiment.

3. Experimental results and analysis

Shown in Figs. 3(a) and 3(b) are the x-ray images from a gasbag and a void half hohlraum, respectively. We also plot in Figs. 3(c) and 3(d) the line profiles of the images along the horizontal line $y = 460$ that passes through the centre of the image. We can see from Figs. 3(a) and 3(d) that the spot size is about 1600 μm, the same as the inner-diameter of the gasbag. The parabola-like intensity profile in Fig. 3(d) is understandable for the gasbag target. The x-rays that can be detected with the x-ray pinhole camera are optically thin. Therefore, the intensity of these x-rays is proportional to the area density of the plasmas, i.e., the integrated electron density along the line of the view. From the top view of the gasbag, the gas area density gradually decreases from the centre to the edge, leading to a higher plasma area density at the image centre when the target is irradiated by the laser beams. Therefore, the x-rays are more intense at the image centre. The consistence between the gas area density and the x-ray intensity from the top view is also an indication of the sufficient heating of the gas. In consequence, a millimeter-size plasma should be produced with the gasbag target. For comparison, the x-ray image from the void hohlraum shows a lower x-ray intensity around the view centre. This is because the plasmas near the inner hohlraum wall have higher density. The spot size in Figs. 3(b) and 3(c) is 650 μm, corresponding to the LEH diameter of the void half hohlraum.

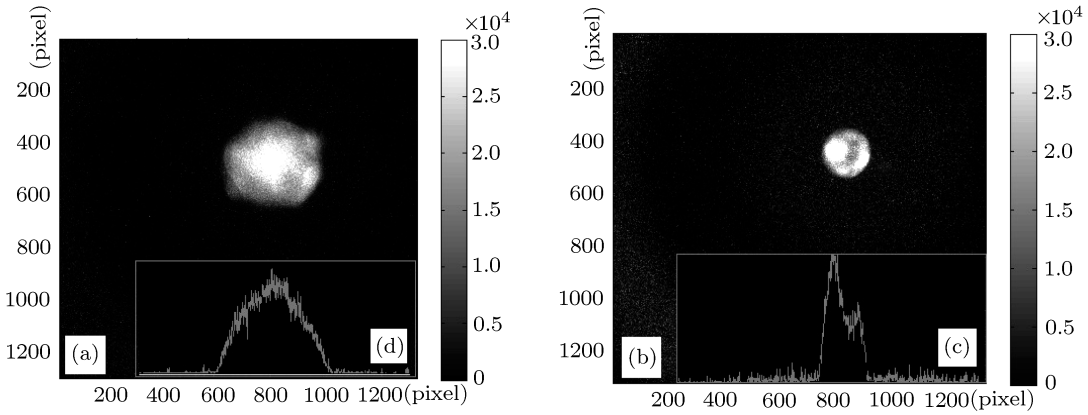


Fig. 3. The x-ray pinhole images of (a) the gasbag and (b) the void half hohlraum. The insets show the line graphs of the intensity profile along the line $y = 460$ of (d) the gasbag and (c) the void half hohlraum.

The SRS spectrum contains rich information of the plasma parameters and hence can be used to infer the electron temperature and density.[9,13] After it was collected with the FABS and transferred through an optical fibre, the back scattered SRS light is dispersed with an optical spectrometer with a focal length of 15 cm and recorded with a streak camera. The wavelength range of the measurement system is 450–650 nm, and the temporal resolution is about 100 ps. Shown in Fig. 4 are the SRS streak spectra scattered from the two types of the targets. In this figure, the wavelength-dependence time delay due to the fibre is already corrected by using the theory investigated by Montgomery *et al.*[18] Shown in Figs. 4(c) and 4(d) are the intensity profiles of the spectra at the time $t = 0.5$ ns. As clearly seen in Fig. 4(a) and Fig. 4(d), the width of the instantaneous SRS

spectrum from the gasbag target is only about 30–40 nm, showing much better uniformity of the millimeter-scale plasmas. As comparison, the bandwidth of the SRS spectrum from the void half hohlraum is about twice that from the gasbag target and is similar to that from planar target,[19,20] indicating a much less uniformity of the plasma produced by the void hohlraum.

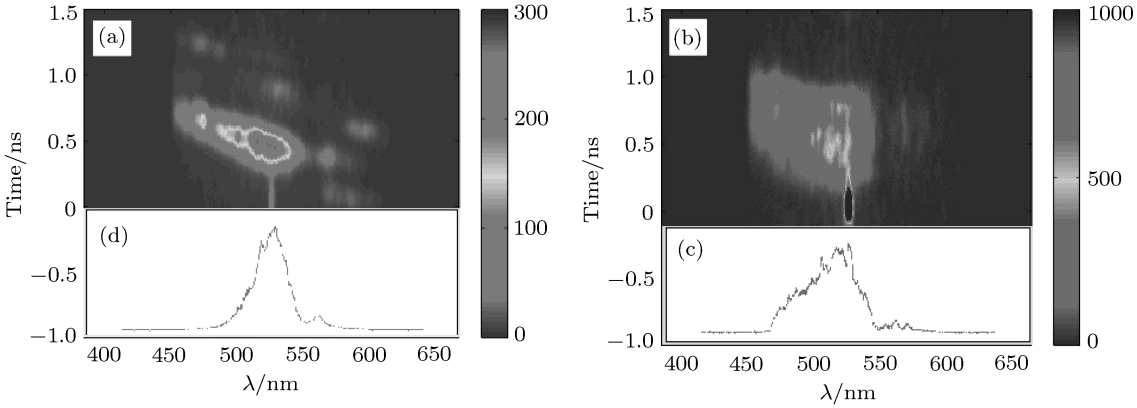


Fig. 4. SRS time-resolved spectrum of (a) the gasbag and (b) the void half hohlraum. The insets show the intensity profile of the spectra at $t = 0.5$ ns of (d) the gasbag and (c) the void half hohlraum.

A simplified model is applied to infer the electron temperature of the Xe plasma in the gasbag target. First of all, the charge state of the Xe plasma is calculated with an average-atomic-model code. The computed results show that the average charge state of Xe varies in the range of 37–42 when the electron temperature generated with 0.8-atm Xe gas is in the range of 1–2 keV. Thus a proper charge state of 40 is chosen for our experimental condition and the estimated electron density of the Xe plasmas is $0.082n_{\rm c}$, where n_c is the critical density of the laser beam. This value is consistent with the electron density inferred from the SRS spectrum. As shown in Fig. 4(a), the initial spectral position of SRS located at 520 nm indicates that SRS takes place in the bulk plasma with an electron density of 0.082 $n_{\rm c}$. In order to obtain the electron temperature, we make use of the equations of matching conditions for SRS[3]

$$\omega_0 = \omega_{\rm s} + \omega_{\rm epw}, \quad \boldsymbol{k}_0 = \boldsymbol{k}_{\rm s} + \boldsymbol{k}_{\rm epw}, \tag{1}$$

where ω_0 is the frequency of the laser beam, $\omega_{\rm s}$ the frequency of the scattered light, $\omega_{\rm epw}$ the frequency of the plasma wave, and $\boldsymbol{k}_0$ is the wave number of the laser beam, $\boldsymbol{k}_{\rm s}$ the wave number of the scattered light, $\boldsymbol{k}_{\rm epw}$ the wave number of the plasma wave. With the dispersion relations of the light waves and electron plasma waves, we can calculate the electron temperature from the matching equations (1) when the electron density is known. By this way, the inferred electron temperature of the Xe plasmas is about 1.6 keV, which is also consistent with the assumed values for the calculation of the charge state.

The time-resolved SRS spectrum of gasbag target is shifted towards shorter wavelength from the time of about 0.5 ns, as seen in Fig. 4(a). The wavelength shift of the SRS spectrum is due to the decreasing plasma density after the time of 0.5 ns. With the assumption that the electron temperature keeps at 1.6 keV in the laser pulse duration, the instantaneous electron density can be inferred through the wavelength of the SRS spectrum by using the matching equations (1). Shown in Fig. 5 is the evolution of the electron density with time that is inferred from the SRS spectrum. We can see that the average electron density is about $0.08n_{\rm c}$ from $t = 0.3$ ns to 0.5 ns, and falls to about $0.035n_{\rm c}$ at $t = 0.85$ ns, where $t = 0$ ns is the beginning of the interaction. This phenomenon could be ascribed to the expansion of the plasma. When the polyimide membrane of the gasbag is irradiated by the laser beams, a shock wave is launched into the target because of the laser ablation, and is immediately followed by a rarefaction wave. Before the arrival of the front of the rarefaction wave, the plasma density keeps to be a constant. After that, the plasma density decreases very quickly.

As seen in Fig. 5, the duration in which the electron density has a flat-platform region is about 200 ps from 0.3 ns to 0.5 ns. This is the efficient time window that the gasbag can offer us to study the large-scale laser-plasma interactions. In our experimental condition, the growth rates of SRS and SBS are about 8×10^{12}/s and 1.5×10^{12}/s, respectively. In the duration of 200 ps, the SRS and SBS instabilities could

develop sufficiently. In these millimeter-scale plasmas,

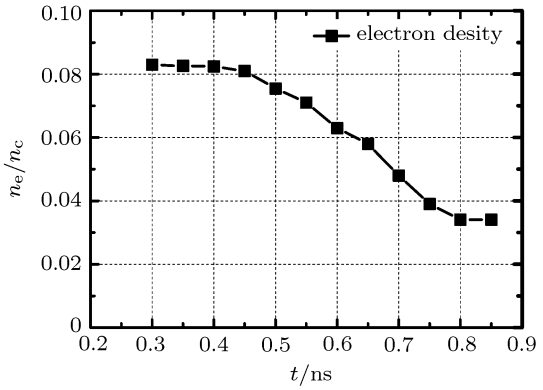


Fig. 5. Electron density versus time inferred from SRS spectrum.

the convection effect is mitigated and the damping rates of the daughter waves may dominate the instabilities. Hence, the LPIs in these millimeter-scale plasmas may partially mimic those in the ignition condition. We then can draw the conclusion that the gasbag target can be used for the research of large-scale laser-plasma interactions.

4. Summary

A gasbag target has been designed and tested to create millimeter-scale plasmas on Shenguang-III prototype laser facility. The x-ray pinhole images show that millimeter-scale plasmas are produced with the gasbag. The electron temperature inferred from the SRS spectrum is about 1.6 keV. The SRS spectrum also indicates that the electron density has a flat region within the duration of about 200 ps. The LPIs in these millimeter-scale plasmas may partly mimic those in the ignition condition. So we conclude that the gasbag target can be used to research large-scale LPIs.

Acknowledgement

The authors are grateful to the target fabrication team and the operation group of Shenguang-III prototype for their laborious work and close collaboration. The authors thank Wu Shun-Chao and Pu Yu-Dong for their valuable discussion.

References

[1] Lindl John 1995 *Phys. Plasma* **2** 2933
[2] Lindl John, Amendt Peter, Berger R L, Glendinning S G, Glenzer S H, Haan S W, Kauffman R L, Landen O L and Suter L L 2004 *Phys. Plasma* **11** 339
[3] Kruer W L 1988 *The Physics of Laser Plasma Interactions* (Redwood City: Addison-Wesley)
[4] Qi L Y, Jiang X H, Zhao X W, Li S W, Zhang W H, Li C G, Zheng Z J and Ding Y K 2000 *Acta Phys. Sin.* **49** 492 (in Chinese)
[5] Hinkel D E, Callahan D A, Langdon A B, Langer S H, Still C H and Williams E A 2008 *Phys. Plasma* **15** 056314
[6] Steveson R M, Suter L J, Oades K, Kruer W, Slark G E, Fournier K B, Meezan N, Kauffman R, Miller M, Glenzer S, Niemann C, Grun J, Davis J, Back C and Thomas B 2004 *Phys. Plasma* **11** 2709
[7] Froula D H, Divol L, London R A, Michel P, Berger R L, Meezan N B, Neumayer P, Ross J S, Wallace R and Glenzer S H 2008 *Phys. Rev. Lett.* **100** 015002
[8] Neymayer Paul, Berger R L, Divol L, Froula D H, London R A, MacGowan B J, Meezan N B, Ross J S, Sorce C, Suter L J and Glenzer S H 2008 *Phys. Rev. Lett.* **100** 105001
[9] Froula D H, Divol L, London R A, Berger R L, Doppner T, Meezan N B, Ross J S, Suter L J, Sorce C and Glenzer S H 2009 *Phys. Rev. Lett.* **103** 045006
[10] Kirkwood R K, Moody J D, Niemann C, Williams E A, Langdon A B, Landen O L, Divol L, Suter L J, Depierreux S and Seka W 2006 *Phys. Plasmas* **13** 082703
[11] Glenzer S H, MacGowan B J, Michel P, Meezan N B, Suter L J, Dixit S N, Kline J L, Kyrala G A, Bradley D K, Callahan D A, Dewald E L, Divol L, Dzenitis E, Edwards M J, Hamza A V, Haynam C A, Hinkel D E, Kalantar D H, Kilkenny J D, Landen O L, Lindl J D, LePape S, Moody J D, Nikroo A, Parham T, Schneider M B, Town R P J, Wegner P, Widmann K, Whitman P, Young B K F, Wonterghem B van, Atherton L J and Moses E I 2010 *Science* **327** 1228
[12] Jiang X H, Zheng Z J, Li W H, Liu Y G, Zheng J and Wang Y C 2000 *High Power Laser and Particle Beams* **12** 48 (in Chinese)
[13] Wang Z B, Zheng J, Jiang X H, Liu S Y, Li W H, Liu W D, Yu C X, Liu Y G, Zhang H Y, Tang X Q, Peng X S, Ding Y K and Zheng Z J 2004 *High Power Laser and Particle Beams* **16** 45 (in Chinese)
[14] Denavit J and Phillion D W 1994 *Phys. Plasmas* **1** 1971
[15] Zhang X M, Zheng W G, Wei X F, Jing F, Sui Z, Su J Q, Li M Z, Zhu Q H, Peng Z T, He S B, Yu H W, Chen B, Jiang X D and Zhou H 2005 *Proc. SPIE* **5627** 6
[16] Li S W, Yi R Q, Jiang X H, He X A, Cui Y L, Liu Y G, Ding Y K, Liu S Y, Lan K, Li Y S, Wu C S, Gu P J, Pei W B and He X T 2009 *Acta Phys. Sin.* **58** 3255 (in Chinese)
[17] Froula D H, Bower D, Chrisp M, Grace S, Kamperschroer J H, Kelleher T M, Kirkwood R K, MacGowan B, McCarville T, Sewall N, Shimamoto F Y, Shiromizu S J, Young B and Glenzer S H 2004 *Rev. Sci. Instrum.* **75** 4168
[18] Montgomery D S and Johnson R P 2001 *Rev. Sci. Instrum.* **72** 979
[19] Ding Y K, Zheng Z J, Tang D Y, Liu S Y, Chen Z L, Mei Q Y, Qi L Y, Li S W, Ding Y N and Liu Z L 1996 *High Power Laser and Particle Beams* **8** 215 (in Chinese)
[20] Jiang X H, Li W H, Liu Y G, Deng W, Ding Y K and Zheng Z J 1998 *Acta Phys. Sin.* **47** 35 (in Chinese)